MOLECULAR AND CELLULAR BIOLOGY, Jan. 2011, p. 190–202 Vol. 31, No. 1
0270-7306/11/$12.00 doi:10.1128/MCB.00317-10

Sequential Recruitment of SAGA and TFIID in a Genomic Response to DNA Damage in *Saccharomyces cerevisiae*[▽]

Sujana Ghosh and B. Franklin Pugh*

Center for Eukaryotic Gene Regulation, Department of Biochemistry and Molecular Biology, The Pennsylvania State University, University Park, Pennsylvania 16802

Received 18 March 2010/Returned for modification 2 June 2010/Accepted 12 October 2010

Eukaryotic genes respond to their environment by changing the expression of selected genes. The question we address here is whether distinct transcriptional responses to different environmental signals elicit distinct modes of assembly of the transcription machinery. In particular, we examine transcription complex assembly by the stress-directed SAGA complex versus the housekeeping assembly factor TFIID. We focus on genomic responses to the DNA damaging agent methyl methanesulfonate (MMS) in comparison to responses to acute heat shock, looking at changes in genome-wide factor occupancy measured by chromatin immunoprecipitation-microchip (ChIP-chip) and ChIP-sequencing analyses. Our data suggest that MMS-induced genes undergo transcription complex assembly sequentially, first involving SAGA and then involving a slower TFIID recruitment, whereas heat shock genes utilize the SAGA and TFIID pathways rapidly and in parallel. Also Crt1, the repressor of model MMS-inducible ribonucleotide reductase genes, was found not to play a wider role in repression of DNA damage-inducible genes. Taken together, our findings reveal a distinct involvement of gene and chromatin regulatory factors in response to DNA damage versus heat shock and suggest different implementations of the SAGA and TFIID assembly pathways that may depend upon whether a sustained or transient change in gene expression ensues.

One way that eukaryotes respond to environmental signals is to change the expression of their genes (4, 13). A plethora of proteins are involved in regulating gene expression, including those that recognize specific DNA sequences, modify or remodel chromatin, assemble the preinitiation complex (PIC), and regulate transcription elongation (33, 40, 43, 44). Both the sequence-specific factors and the general transcription machinery might vary in composition depending upon the signaling events that are involved (6, 15, 17, 26, 34). However, beyond the role of different sequence-specific factors, it remains unclear to what extent the downstream events in the transcription cycle are uniform or specialized when an organism is exposed to different environmental conditions.

The heat shock and DNA damage response pathways are two well-studied model systems for understanding the steps in the transcription cycle (47, 49, 50). In *Saccharomyces cerevisiae*, heat shock, DNA damage, and many other environmental stresses/signals induce a common set of environmental stress response (ESR/CER) genes (12, 13). However, the response to DNA damaging agents creates an additional genomic response profile that is not found with other stresses. In particular, cell cycle arrest occurs and the DNA damage repair pathway is induced. Unlike the transient heat shock response, the response to DNA damage is sustained for many hours (9, 11, 12, 18, 46). Induction of ESR/CER genes by DNA damaging agents is attenuated in strains in which the DNA damage repair signaling pathway (i.e., *MEC1* and *DUN1*) is disrupted, but the same genes are properly induced in response to heat shock (12). This suggests that distinct signaling pathways converge to activate a common set of genes. Thus, these two systems represent suitable models for ascertaining the extent to which the mechanics of a transcriptional response can differ or be similar when cells are exposed to conditions which invoke common as well as stress-specific responses.

The study of the heat shock response in addition to previous work has corroborated the finding of two mutually compatible pathways for PIC assembly (19, 22, 25, 29, 39). One involves SAGA-directed PIC assembly through genes that contain a TATA box and bind a TAF-free form of TATA binding protein (TBP). Such genes represent only about 10 to 20% of all yeast genes and tend to be stress induced and subjected to widespread inhibition by repressors of chromatin and PIC assembly. In contrast, the TFIID-directed pathway of PIC assembly tends to dominate at TATA-less genes, which comprise 80 to 90% of the yeast genome. These genes tend to be housekeeping genes that are expressed at constitutively low levels, except in the case of the ribosomal protein (RP) genes. These pathways are compatible in that loss of one can be compensated partially by the other. Additionally, many genes are occupied by various levels of both SAGA and TFIID. For example, RP genes contain high levels of both TFIID and SAGA (32). Moreover, both SAGA and TFIID are recruited to heat shock-induced genes (50).

Repression and induction of DNA damage response genes have been studied primarily with the *RNR2*, *-3*, and *-4* and *HUG1* genes (18, 55). At these genes, Crt1 binds to its recognition motif and recruits the chromatin repression complex SSN6-TUP1, as well as histone deacetylases to maintain genes in a repressed state (18, 27, 37). The DNA damaging agent methyl methanesulfonate (MMS) has been used to study induction (20). Damage sensing and induction occur through a

* Corresponding author. Mailing address: Department of Biochemistry and Molecular Biology, The Pennsylvania State University, 456 North Frear Laboratory, University Park, PA 16802. Phone: (814) 863-8252. Fax: (814) 863-7024. E-mail: bfp2@psu.edu.

▽ Published ahead of print on 18 October 2010.

Mec1p-Rad53p-Dun1p protein kinase pathway (9, 45, 54) which ultimately leads to Crt1 phosphorylation and release from repressed promoters.

In addition to repression, Crt1 is also thought to function as an activator of the *RNR* genes during MMS induction by directly or indirectly facilitating the recruitment of TFIID and SWI/SNF (36, 52, 53), which in turn promote chromatin remodeling and full assembly of the preinitiation complex. Such retention of Crt1 would seem to contradict findings that Crt1 dissociates when target genes are activated. It is conceivable that Crt1 is retained at the promoter at least until the commitment to recruit TFIID and/or SWI/SNF is made. Thus, whether the release of Crt1 from the model *RNR3* promoter is immediate or delayed upon MMS treatment is unclear, at least for the early stages of induction.

While the repression of *RNR* genes by Crt1 has long been considered a model for the regulation of DNA damage-inducible genes, very few MMS-induced genes have been associated with Crt1-directed repression (12, 18). This may be due in part to limited genome-wide studies that specifically address this problem. Using custom-made oligonucleotide arrays, we have now generated moderate-resolution tiling array occupancy data for Crt1 before and after MMS treatment. We also examined the genome-wide distribution of its corepressor SSN6-TUP1, its coactivators SWI/SNF and TFIID, and other general transcription factors (GTFs) and sequence-specific regulators that may be part of the MMS response.

By comparing the genome-wide distribution of a wide range of factors in response to DNA damage to the distribution during the heat shock response, we have taken some initial steps toward understanding whether distinct environmental response pathways interface with the transcription cycle in the same or a distinct manner. Surprisingly, we found that while the heat shock pathway involves the simultaneous deployment of the TFIID-dominated and SAGA-dominated PIC assembly pathways, the response to MMS initially involves SAGA recruitment and not TFIID. However, SAGA is ultimately replaced by TFIID, suggesting that genes utilize the stress-related SAGA pathway to mount an immediate transient response and then follow up with the TFIID housekeeping pathway for a long-term response.

In addition to DNA damage, MMS is destructive toward proteins, resulting in their turnover and ultimately in the biosynthesis of amino acids to resynthesize the proteins. Gcn4 is a master regulator of amino acid biosynthetic genes (31). Indeed, we found that Gcn4 is recruited to amino acid biosynthetic genes in response to MMS but not in response to heat shock, and this is linked to the recruitment of the SAGA complex, in accord with known interactions between Gcn4 and SAGA (2, 7, 10, 41).

MATERIALS AND METHODS

Yeast strains, growth conditions, and public data sets. *Saccharomyces cerevisiae* S288C strains were obtained from a yeast tandem affinity purification (TAP) fusion library (Open Biosystems). C-terminally TAP-tagged proteins were immunoprecipitated using IgG antibodies. Untagged strain BY4741 was used for null chromatin immunoprecipitation (ChIP) and as a control for occupancy normalization.

Each strain was grown to an optical density at 600 nm (OD_{600}) of 0.8 at 25°C in 500 ml of yeast extract-peptone-dextrose (YPD). MMS was then added to a final concentration of 0.03% for 30 min, 1 h, or 2 h for DNA damage growth conditions. For heat shock conditions, cultures were heat shocked at 37°C for 15 min (or 5 min) or mock treated at 25°C for 15 min (or 5 min) by adding volumes of appropriately heated medium to achieve the desired final temperature.

Where indicated, published gene expression data for DNA damage were from the work of Gasch et al. (12) (expression data sets for 30 min and 2 h of exposure to 0.02% MMS were used). Gene expression data for 15 min of heat shock were from the work of Zanton and Pugh (49). Expression data sets for 5 and 15 min of heat shock were from the work of Gasch et al. (13). ChIP-microchip (ChIP-chip) data for heat shock conditions for the factors Rpo21, Taf1, Sua7, Ssl2, Spt3, Ino80, and Isw1 were from the work of Venters and Pugh (43).

ChIP-chip and microarray expression assays. ChIP assays were performed as described previously (49). Following treatment (respective stress and mock stress), cells were cross-linked with 1% formaldehyde for 15 min at 25°C and then quenched for 5 min with glycine. After being harvested, the cells were lysed with zirconium beads, and the washed chromatin pellet was sheared by sonication using a Bioruptor (Diagenode), generating, on average, 200- to 300-bp DNA fragments. Sheared chromatin was immunoprecipitated with IgG-Sepharose, and the ChIP-enriched DNA was then amplified using ligation-mediated PCR (LM-PCR) (15). LM-PCR-amplified DNA fragments (75 to 300 bp) were gel purified using a Qiagen protocol. DNA yields following gel purification were determined using a Nanodrop ND-1000 spectrophotometer.

DNA labeling and hybridization to the custom oligonucleotide tiling arrays were performed as described previously (49). One hundred nanograms of gel-purified, LM-PCR-amplified, ChIP-enriched DNA was amplified by 15 PCR cycles. The MMS-treated and 37°C samples were then Cy5 labeled, and the MMS-untreated and 25°C samples were Cy3 labeled and cohybridized to microarrays. A dye swap was performed with independent biological replicates for every factor.

For expression analysis, BY4741 cultures were treated as described above for the respective stress conditions (DNA damage or heat shock), and the cells were harvested at the end of the treatment. Sample preparation and microarray assays were performed as described in previous publications (5, 19). Changes in gene expression were similar to published results (12, 13).

Array design and analysis. The array design for the low-density tiling microarrays was the same as that described previously (43). Occupancy data were filtered, normalized to corresponding probes in the null (no-tag) control, centered by dividing the data by the median normalized probe value for those probes located in intergenic regions between two convergent genes, and $\log_2$ transformed as described previously (50). For changes in occupancy, ratios were calculated with filtered signals, $\log_2$ transformed, and centered by subtracting the median ratio for probes located in intergenic regions between two convergent genes. CLUSTER and TREEVIEW were used for analysis and representation of microarray data (8). *P* values were calculated by using the CHITEST function in Excel.

ChIP-seq assays. ChIP-sequencing (ChIP-seq) assays were performed as described previously (49). Library preparation was done according to the Applied Biosystems SOLiD protocol, using ChIP-enriched DNA, with individual samples bar coded using multiplexed 4-bp adaptors. They were then pooled together and sequenced using a SOLiD sequencer. Thirty-one-base-pair sequence reads were then aligned back to the reference yeast genome by use of SHRiMP software, allowing up to 3 mismatches (35). A summary of the sequencing tag counts is presented in Table 1.

Microarray data accession numbers. Raw data are accessible through ArrayExpress (accession number E-MEXP-2614), and processed data are available at http://atlas.bx.psu.edu/project/saccharomyces.html. Raw ChIP-seq tags are available at NCBI Trace Archives (accession number SRA024321).

RESULTS

Differential recruitment of TFIID to MMS-induced versus heat shock-induced promoters. Genome-wide measurements of factor occupancy levels were measured by ChIP-chip assay, using a custom array platform in which three oligonucleotides were arrayed for each gene: one in the vicinity of where upstream activation sequences (UASs) tend to reside, one in the vicinity of the core promoter, and one internal to the gene open reading frame (ORF), near its 3′ end (43). In addition, several hundred locations were arrayed in intergenic regions between two convergently transcribed genes and were used as background controls. The array contained a total of ~20,000

TABLE 1. ChIP-seq tag counts

Sample	No. of uniquely aligned tags	T-T median tag count	Normalization factor
Taf1 −MMS 2h1	1,835,945	57	3.56
Taf1 +MMS 2h1	1,311,384	36	2.25
Taf1 −MMS 1h1	3,600,939	72.5	4.53
Taf1 +MMS 1h1	740,322	21	1.30
Taf1 −MMS 30m1	636,523	19	1.18
Taf1 +MMS 30m1	2,683,833	79.5	4.97
Taf1 −MMS 2h2	1,556,167	37	2.31
Taf1 +MMS 2h2	2,046,087	48	3.00
Taf1 −MMS 1h2	3,885,845	85	5.31
Taf1 +MMS 1h2	1,382,606	36	2.25
Taf1 −MMS 30m2	1,528,003	41	2.56
Taf1 +MMS 30m2	2,560,351	71.5	4.47
Taf1 mock HS 15m1	1,409,985	33	2.06
Taf1 HS 15m1	1,553,850	33	2.06
Taf1 mock HS 5m1	2,117,035	19	1.19
Taf1 HS 5m1	819,909	36	2.25
Taf1 mock HS 15m2	1,039,450	25	1.56
Taf1 HS 15m2	1,697,294	35	2.19
Taf1 mock HS 5m2	929,677	30	1.88
Taf1 HS 5m2	1,375,176	51	3.19
Spt3 −MMS 2h1	2,874,711	83	5.19
Spt3 +MMS 2h1	1,085,071	34	2.13
Spt3 −MMS 1h1	959,897	30	1.88
Spt3 +MMS 1h1	539,541	16	1.00
Spt3 −MMS 30m1	1,903,997	57	3.56
Spt3 +MMS 30m1	1,287,958	39	2.44
Spt3 −MMS 2h2	1,674,694	51	3.19
Spt3 +MMS 2h2	1,114,933	34.5	2.16
Spt3 −MMS 1h2	1,613,405	49.5	3.09
Spt3 +MMS 1h2	1,519,166	44	2.75
Spt3 −MMS 30m2	1,902,779	56	3.50
Spt3 +MMS 30m2	1,648,994	50.5	3.16
Spt3 mock HS 15m1	2,157,762	55	3.44
Spt3 HS 15m1	852,461	31	1.94
Spt3 mock HS 5m1	2,207,208	54	3.38
Spt3 HS 5m1	1,228,132	20	1.25
Spt3 mock HS 15m2	2,531,648	48	3.00
Spt3 HS 15m2	1,360,396	35	2.19
Spt3 mock HS 5m2	1,820,703	23	1.44
Spt3 HS 5m2	1,430,151	32.5	2.03

probes. The two promoter-proximal probes allowed detection of factor binding from about position −400 to about position +100 relative to the start of each open reading frame.

Occupancies were compared under normal (YPD medium, 25°C) conditions as well as after a 30-min treatment with 0.03% MMS. Expression profiles of mRNAs were also generated, which exactly reproduced those published earlier (12). Occupancy and mRNA changes were also compared under acute heat shock conditions (15 min at 37°C), as these were the conditions employed in studies that defined the genomic heat shock response (4, 13). Genes that responded to the two stresses were largely distinct (Fig. 1A), although there was significant overlap in the two responses, in accord with previous studies (12–14). We first focused on induced genes, then on repressed genes, and finally on those that were neither induced nor repressed but contained significant factor occupancy under one condition or both.

We first compared the utilization of the TFIID versus SAGA pathway and included other representatives of the GTFs. As shown by the cluster plot in Fig. 1B, genes could be separated in accordance with changes in gene expression and matched with corresponding changes in occupancy levels. Genes induced by MMS (left panel, cluster 1) acquired GTFs (TFIIB/Sua7, TFIIH/Ssl2, and Pol II), as expected. Surprisingly, these genes acquired SAGA (Spt3) but not TFIID (TAF1), despite apparent results to the contrary for the model MMS response gene *RNR3* (51, 52). This also contrasts with the response obtained for heat shock (Fig. 1B, right panel, cluster 1), in which heat shock-induced genes acquired both TFIID and SAGA, as shown previously (49, 50). Quantification of occupancy changes between MMS-induced and heat shock-induced genes is shown in Fig. 1C. Note that the absolute scales between different factors are less comparable, due to intrinsic differences in cross-linking efficiency, than comparisons for the same factor under MMS and heat shock conditions. Thus, TAF1 was not substantially recruited to MMS-induced genes compared to heat shock-induced genes.

The general lack of acquisition of TFIID upon MMS induction might have a number of explanations: (i) the previously observed phenomenon might have been specific to a few genes, such as *RNR3*; (ii) TFIID might already be present, and thus no additional acquisition would occur; or (iii) the timing of TFIID acquisition may be slow, such that we failed to detect its presence after 30 min of MMS treatment. Previous studies examined TFIID occupancy after 2 h of treatment with MMS (51, 52).

To address whether TFIID is loaded specifically on the *RNR* genes in response to MMS or is constitutively present and unchanging at most MMS-induced genes, we quantified TFIID (TAF1) and other GTF occupancies at *RNR2*, *-3*, and *-4*, as well as at the MMS-induced cluster 1 genes, before and after MMS treatment (Fig. 2). These occupancies represent the component values by which changes in occupancy were calculated for Fig. 1. For purposes of assessing dynamic range within the data set, median occupancy levels for lowly and highly expressed genes (bottom and top 10 percentiles of transcription frequency [17]), as well as the highly active RP genes, are shown. In addition, for purposes of comparison to an expected level of occupancy for inducible genes, we examined the collection of heat shock-induced genes in response to heat shock (heat shock cluster 1).

RNR2, *RNR4*, and the median for MMS-induced genes displayed similar levels of low GTF occupancy before induction by MMS and a similar magnitude of change after induction to that seen at heat shock-induced genes in response to heat shock (Fig. 2A to C; note that the background levels associated with the *RNR3* "TSS" probe might reflect a probe defect). The SAGA level appeared to be constitutively high at heat shock-induced genes and at intermediate levels at MMS-induced genes, in contrast to its dynamic range (Fig. 2D; note that the "UAS" probe was used and may be positioned improperly at *RNR4*, as illustrated in Fig. 4C). Its level increased modestly in response to MMS or heat shock induction. In contrast, TFIID levels were low prior to induction of both classes of genes (Fig. 2E) but remained low at the MMS-induced genes after induction, whereas relatively high levels of recruitment were apparent at heat shock-induced genes upon induction. Thus, SAGA may be present constitutively at inducible genes, whereas TFIID is immediately recruited to the heat shock genes but not to MMS-induced genes.

We next compared TFIID occupancy levels at 0.5 and 2 h of

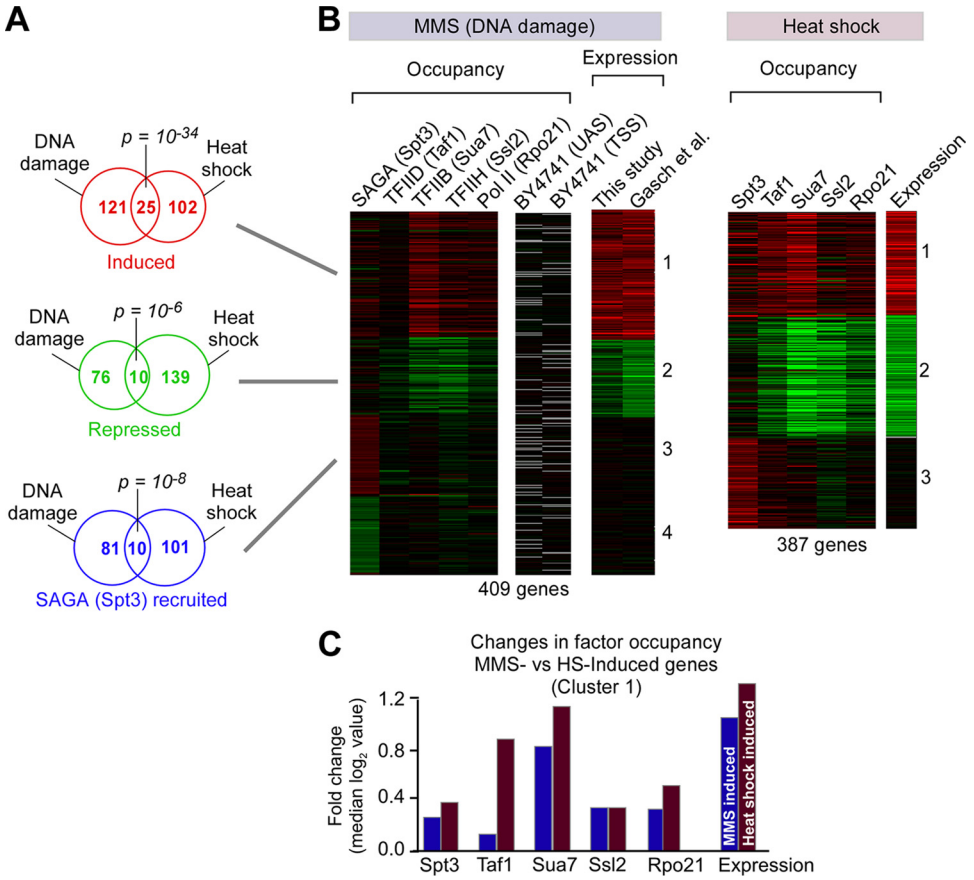

FIG. 1. Changes in factor occupancy in response to 30 min of MMS treatment in comparison to a heat shock response. (A) Venn diagram illustrating the gene membership overlap for genes in equivalently labeled clusters in panel B. (B) Cluster plots of changes in factor occupancy and gene expression (as indicated). MMS-treated and heat shock-treated data sets were clustered separately. Data were filtered to retain only those having 100% data present and >1.5-fold changes in occupancy in at least one data set. The numbers of genes meeting such criteria are indicated. Data were clustered by *K* means ($K = 4$ for MMS and $K = 3$ for heat shock). BY4741 represents a negative control in which the untagged parental strain was processed through the standard TAP-ChIP procedure. Data shown are for the "UAS" and "TSS" microarray probes. The Spt3 ChIP data set used the "UAS" probe, whereas the remaining factors used the "TSS" probe. (C) Median $\log_2$ values for data sets in cluster 1.

induction, with the latter being the time point when TFIID occupancy was previously detected (51, 52). Interestingly, TFIID occupancy increased over the time course, whereas SAGA occupancy increased initially and then decreased back to the uninduced levels (Fig. 3A). Thus, our inability to initially detect TFIID occupancy may be due to delayed recruitment. Importantly, these results suggest that MMS-induced promoters may transition from an early, SAGA (Spt3)-regulated state to a more constitutive, TFIID (TAF1)-regulated state later on. This contrasts with their apparently simultaneous recruitment to heat shock-induced genes. Simultaneous recruitment might be due to the fact that the heat shock response is more transient and more robust than the response to MMS, and thus heat shock genes may need to deploy SAGA and TFIID more quickly. The MMS response, being more sustained, might therefore deploy the SAGA "emergency" response early and the sustainable TFIID response over the long haul.

Given the differences in the physiological and kinetic natures of the two responses, where the heat shock response is a very rapid response and the DNA damage response is a delayed response, it can be argued that the comparison between TFIID and SAGA was done when the heat shock response was in its decline (at 15 min), whereas the DNA damage response was on the rise (at 30 min). Thus, the differences seen in the recruitment of TFIID might actually be due to the differences in timing at which the localization was monitored.

To obtain a more refined time course, we performed ChIP-seq analysis of Taf1 and Spt3 in the presence and absence of MMS for 0.5, 1, and 2 h. For heat shock, two time points, 5 and 15 min, were used along with mock heat shock for the same periods. Biological replicates were generated for each condition and every time point. ChIP material was subjected to deep sequencing, using an AB SOLiD genome sequencer.

Median tag counts were first calculated for ~1,089 intergenic regions between two convergently transcribed genes ("T-T" regions). Little binding was expected in these regions due to the lack of a promoter, thus reflecting the background. Data sets were then scaled to achieve an equal background (median T-T value), inasmuch as the total number of acquired tags is a property of the sequencing process rather than having a biological basis. Changes in occupancy (tag counts) in response to MMS or heat shock were then calculated as ratios relative to mock treatment. Biological replicates were well correlated and thus were averaged.

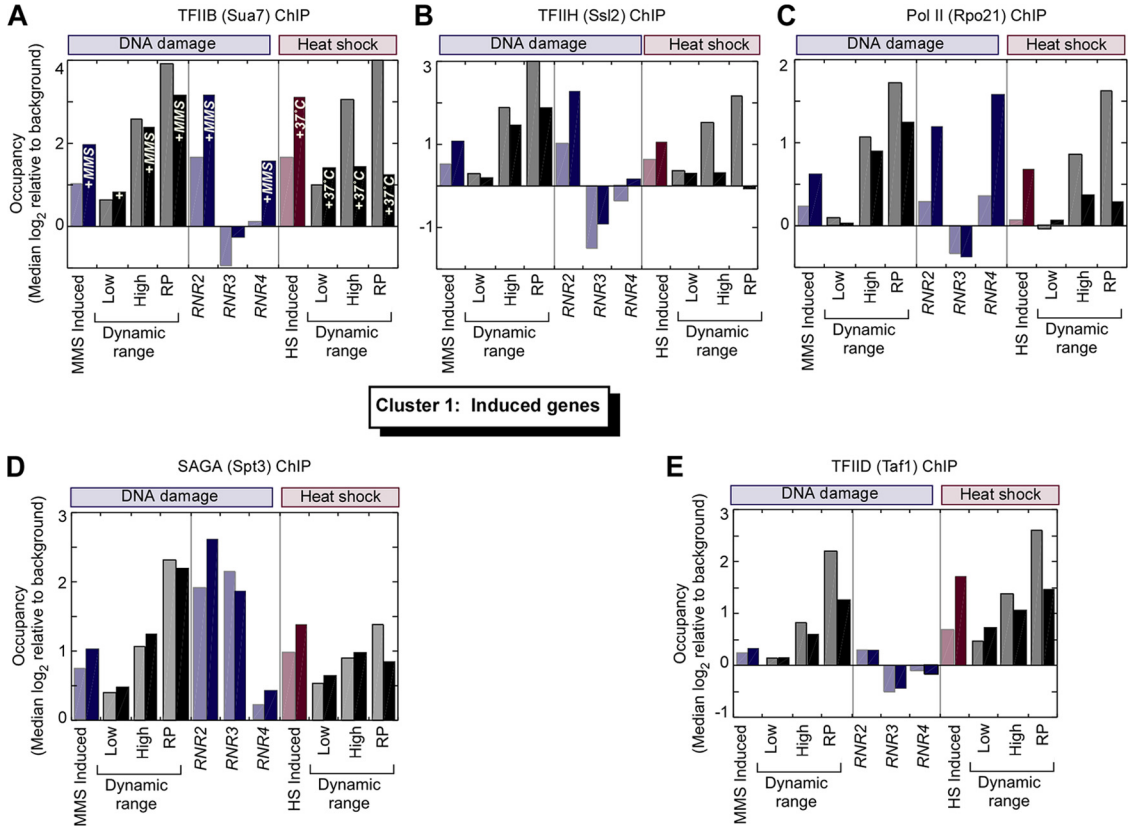

FIG. 2. Factor occupancy levels at *RNR* genes and MMS-induced genes in comparison to heat shock-induced genes. (A to E) Each panel tracks the indicated GTF and reports the median occupancy level for the indicated gene or set of genes. Values represent medians for cluster 1 data, represented as $\log_2$ fold changes over background in the presence or absence of MMS or heat shock, as indicated. The same data used to plot fold changes in occupancy for Fig. 1 were used here. "Low" and "high" represent the bottom and top 10th percentiles of transcription frequency, as defined by Holstege et al. (17). "RP" denotes ribosomal protein genes. The "TSS" probe was used for all data except for the SAGA data, for which the "UAS" probe was used, which is where SAGA is thought to bind (23, 43). For the *RNR4* gene, the "UAS" probe was used instead of the "TSS" probe because it was located closer to the known core promoter region. This places it out of range of where SAGA might be expected to bind. The absence of a significant signal from the *RNR3* TSS probe (used for Sua7, Taf1, and Rpo21) may be due to a defect in the probe. Values for the *RNR* genes represent the averages of two measurements, whereas values for gene sets represent median values of >200 measurements (two replicates of >100 genes) and thus are more robust.

In response to MMS, SAGA recruitment increased after 30 min, remained steady through 1 h, and then dropped precipitously by 2 h of MMS induction (Fig. 3B). In contrast, TFIID occupancy remained low through 1 h and then increased robustly by 2 h of MMS treatment. Throughout this time, expression levels stayed constant (Fig. 3C), indicating that the transition from SAGA- to TFIID-supported transcription had a minimal effect on mRNA output.

Heat shock, on the other hand, showed simultaneous recruitment of TFIID and SAGA at 5 min and through 15 min of exposure (Fig. 3D). Strikingly, 5 min of heat shock resulted in more recruitment of both SAGA and TFIID than did 15 min of heat shock. Transcript levels, however, continued to increase slightly (Fig. 3E), consistent with the well-established peak of the transient heat shock response at 15 min of exposure (4, 13). The combined set of ChIP-chip, ChIP-seq, and expression data suggests that the sustained DNA damage response involves a transient SAGA-directed PIC assembly, which is replaced by TFIID-directed PIC assembly. In contrast, the rapid and transient heat shock response is characterized by a transient and parallel deployment of both the SAGA- and TFIID-directed pathways.

Unexpected mobilization and retention in response to stress of factors that are not coupled to a transcriptional response. We next examined MMS-repressed genes. Like heat shock-repressed genes, which tend to be TFIID dominated, we saw a loss of the GTFs (including TFIID) upon MMS treatment, although their initial levels were relatively low, as is typical of housekeeping genes (Fig. 4A). This is consistent with the notion of a common PIC pathway for housekeeping genes that is shut down during a stress response. We did not see a loss of SAGA from repressed promoters, whether responding to MMS or to heat shock. Conceivably, the retention of SAGA might contribute to the reestablishment of transcription of these genes once the stress has been alleviated, although this remains to be tested.

For both MMS-treated and heat-shocked cells, we observed a third type of gene cluster (cluster 3) in which SAGA (Spt3) occupancy increased upon treatment (Fig. 4B). These SAGA-recruited genes were generally distinct in the two responses

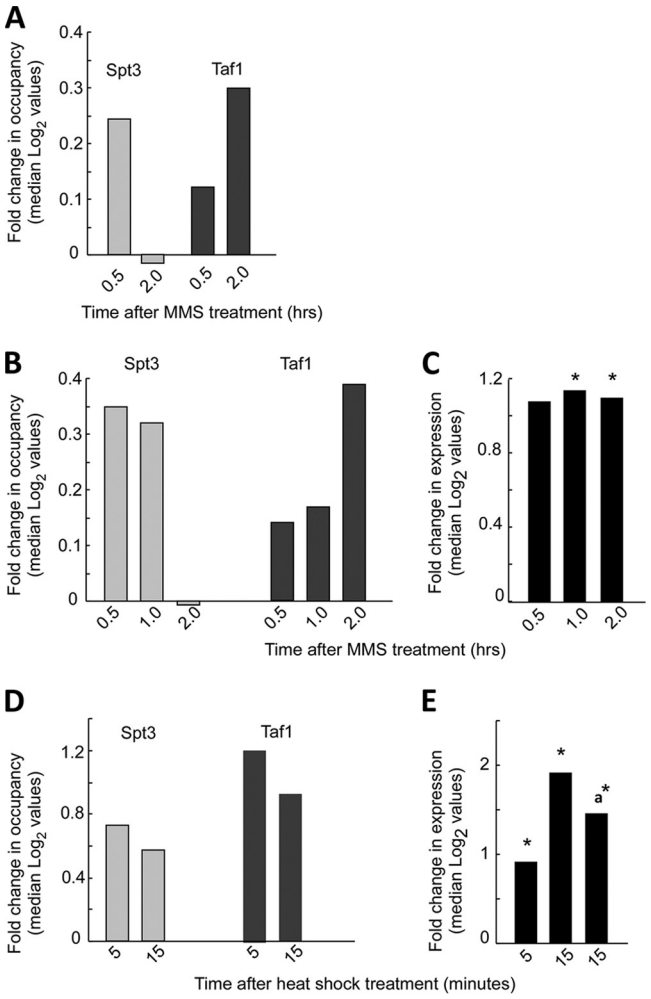

FIG. 3. Delayed acquisition of TFIID at MMS-induced genes, as opposed to simultaneous acquisition of TFIID and SAGA at heat shock-induced genes. (A) Genome-wide Spt3 and Taf1 occupancy changes (ChIP-chip) after 0.5 and 2 h of MMS induction for MMS-induced genes (cluster 1). (B) Changes in occupancy (ChIP-seq) of Spt3 and Taf1 after 0.5 h, 1 h, and 2 h of MMS induction at the MMS-inducible genes. (C) Corresponding changes in mRNA levels are shown. *, the expression data are from the work of Gasch et al. (12). (D) Changes in occupancy (ChIP-seq) of Spt3 and Taf1 following heat shock induction for 5 and 15 min at heat shock-inducible genes. (E) Corresponding changes in mRNA are shown. *, expression data are from the work of Gasch et al. (13); a*, expression data are from the work of Zanton and Pugh (50).

(Fig. 1A). They were lowly expressed and had low to moderate levels of Pol II and TFIIH. The heat shock-defined set had relatively high levels of TFIID and TFIIB that did not change with MMS treatment. This may be equivalent to partial PIC assembly, which was described previously (50). The same was not observed for cluster 3 genes defined by MMS treatment. Gene ontology analysis did not reveal any functional grouping of these genes. While we do not know the basis for these seemingly innocuous changes in SAGA occupancy, they do not seem to be coupled to transcription, nor is the phenomenon stress specific. As reported before (50), the genome undergoes a number of coordinated factor occupancy changes in response to stress, without any apparent or immediate effect on transcription. Nonetheless, regulation in the genome is plastic and perhaps rearranges factors that might help the cell to contend with other stresses that might be linked to and occur subsequent to the primary stress.

Crt1 is not linked to MMS-induced genes. Given the historical focus on a select set of model genes (*RNR2*, *-3*, and *-4*) to decipher MMS derepression mechanisms, we mapped the genome-wide locations of other factors connected to MMS derepression. In particular, we examined Crt1 and its corepressor Tup1 (9, 18, 27). Crt1 reportedly binds to the sequence T(C/T)GCCATGGCAAC (48) and recruits the chromatin corepressor Tup1 (55). At least at the *RNR* genes, Crt1 and Tup1 ultimately dissociate upon DNA damage by MMS (9, 18, 27, 53), and this results in derepression of *RNR* gene expression. This mechanism deduced for the *RNR* genes is a model for the regulation for DNA damage-inducible genes.

We addressed the validity of our Crt1 and Tup1 ChIP-chip data in four ways. First, we examined all regions significantly bound by Crt1 by using MEME and found that it identified the canonical Crt1 site as a highly enriched motif (E value = 7.4×10^{-7}) (Fig. 5A). Thus, our Crt1 ChIP data set has high specificity for its previously defined cognate site. Second, we determined the genome-wide overlap of the top 100 loci with significantly bound Crt1 and the top 250 loci with significantly bound Tup1 (Fig. 5B). A very strong overlap of bound regions was observed ($P < 10^{-65}$). Thus, Crt1 linkage to Tup1 is widespread and robust. Third, we examined Crt1 and Tup1 occupancy at the *RNR* genes. As shown in Fig. 5C, Crt1 and Tup1 were detected by ChIP-chip analysis at *RNR2* and *RNR3*, as expected. Little was detected at *RNR4*, but this might be due to the fact that the probes for *RNR4* were not at an optimal location (illustrated in Fig. 5C). Fourth, upon MMS induction, Crt1 is reportedly depleted at the *RNR* genes (18, 51, 52). At *RNR2* and *RNR3*, we indeed saw a reduction of Crt1 upon MMS treatment, although the amount of depletion was rather modest (1.5- to 2-fold). Together, these findings validate the Crt1 and Tup1 data sets (beyond the standard metrics of reproducibility).

We evaluated Crt1 occupancy at MMS-induced genes as well as at the top 100 Crt1-bound locations for purposes of comparison. Surprisingly, the median occupancy level of Crt1 at MMS-induced genes was rather low, and this did not change with MMS induction (Fig. 5D). Similarly, Tup1 levels were low at MMS-induced genes and did not change upon MMS induction. When we examined the overlap between Crt1-bound genes and MMS-induced genes, only four genes overlapped ($P = 0.8$) (Fig. 5E). A similar low level of overlap was seen with Tup1. However, the few overlapping genes did include the *RNR* genes. Thus, Crt1 and Tup1, despite being present at *RNR* genes and behaving as previously reported, do not appear to have a widespread linkage to the MMS-induced DNA damage response.

Chromatin remodelers are present constitutively at DNA damage-inducible genes. ATP-dependent chromatin remodelers play important roles in repression and activation of DNA damage-inducible genes (3, 30, 36). We therefore examined the genomic distribution of several remodeling complexes, including RSC (Rsc2), SWI/SNF (Snf2), INO80 (Ino80), and ISW1, at bulk MMS-inducible genes, as well as the *RNR* genes, in response to MMS and heat shock (Fig. 6). For purposes of

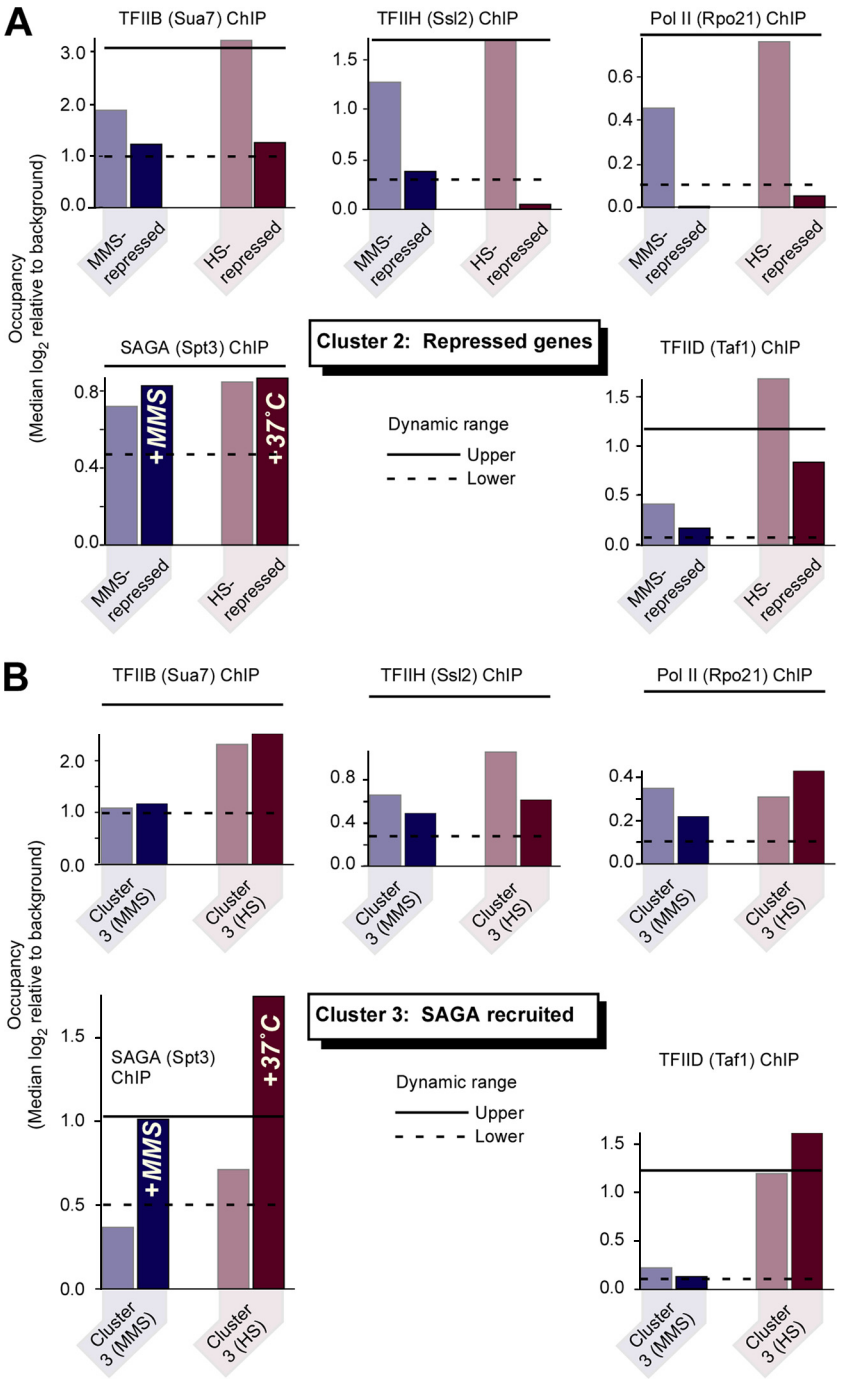

FIG. 4. Occupancy levels at genes that are repressed or unaffected by MMS or heat shock. Occupancy levels are reported for genes in cluster 2 (A; repressed or downregulated) and cluster 3 (B; genes that acquire SAGA but are not immediately activated), as described in the legend to Fig. 2.

setting the dynamic range, we also plotted the apparent occupancy levels at the top 5th and bottom 50th percentiles for all genes (more than half of all genes are expected to have background levels of occupancy). In general, moderately high levels of the RSC, SWI/SNF, and INO80 remodeling complexes were present at MMS-inducible genes prior to and subsequent to induction. The ISW1 complex appeared to be absent from promoter regions of MMS-induced genes. With the exception of SWI/SNF, these remodelers appeared to be absent from *RNR4*, although we cannot exclude the likely possibility that the *RNR4* probes were not in a proper position to detect occupancy. We also detected high-level occupancy of ISW1 at *RNR3*. Since the bulk MMS-induced genes have substantial gene membership, the collective bulk assessment of occupancy at these genes should not be affected by a small number of out-of-position probes.

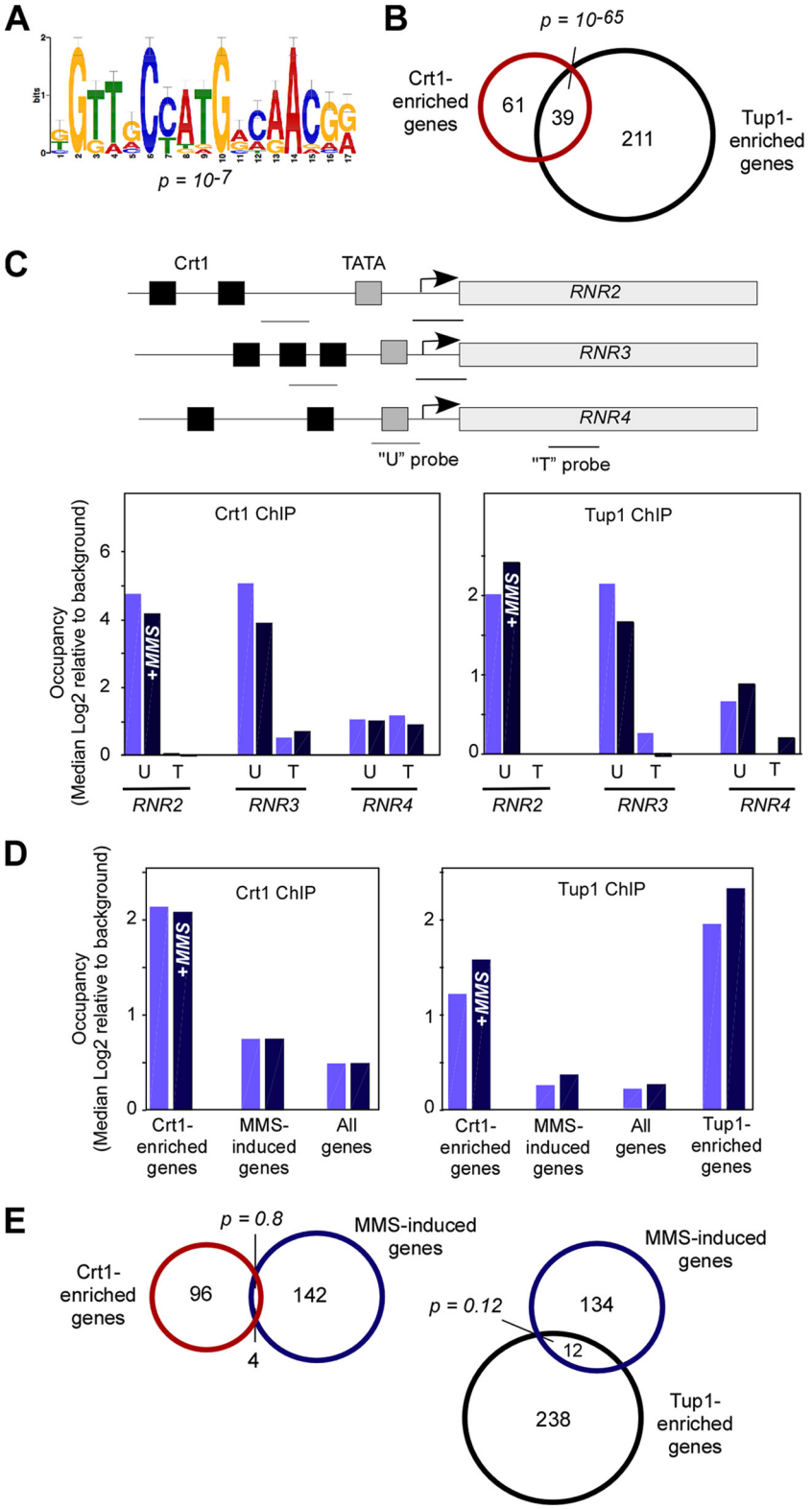

FIG. 5. Crt1 is not linked to MMS-induced genes. (A) Crt1 motif, obtained using MEME, for the significantly bound genes. (B) Venn diagram illustrating the overlap between Crt1- and Tup1-enriched genes genome-wide. Only the topmost 100 Crt1-occupied genes and the topmost 250 Tup1-occupied genes were used. Genes with lower measured occupancy levels of these factors (false-negative results) became less distinguishable from false-positive results and thus were not used. Such stringent filtering would therefore limit the degree of overlap. (C) Bar graph representing Crt1 and Tup1 occupancy, represented as $\log_2$ fold changes over background in the presence or absence of MMS at *RNR* genes. UAS and TSS probe distributions along with Crt1 X-box sites at the *RNR2*, *RNR3*, and *RNR4* genes are shown. (D) Bar graph illustrating Crt1 and Tup1 occupancies, represented as $\log_2$ fold changes over background in the presence or absence of MMS at MMS-inducible genes. Data shown are for the "UAS" microarray probes. (E) Venn diagram representing the overlap between MMS-inducible genes (defined in the legend to Fig. 1A and B) and the Crt1- and Tup1-enriched genes.

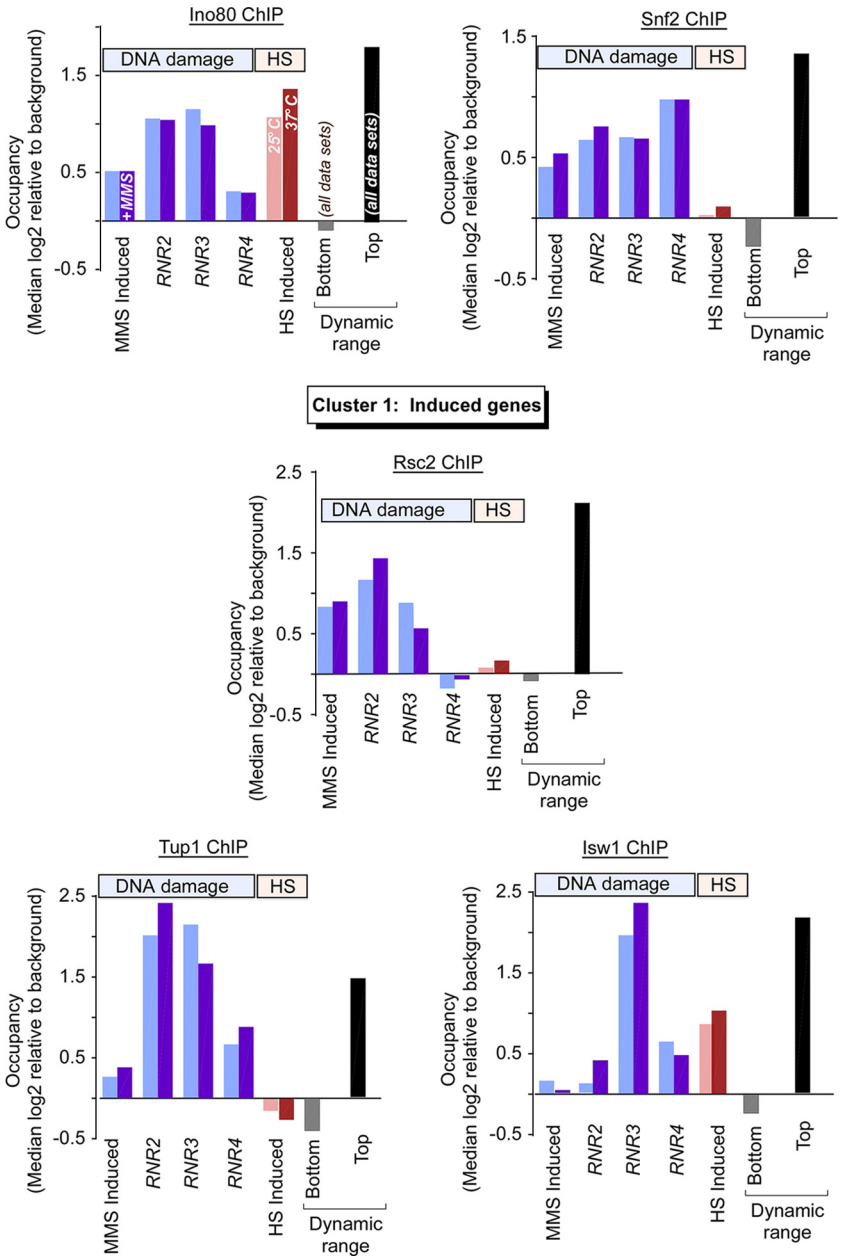

FIG. 6. Constitutive presence of many chromatin remodelers at DNA damage-inducible genes. Each panel tracks the indicated chromatin remodeler and reports the median occupancy levels at the "UAS" probe for the MMS- and heat shock-inducible genes along with the *RNR* genes. Median occupancy values are represented as $\log_2$ fold changes over background in the presence or absence of MMS or heat shock, as indicated. The occupancy levels at the top 5th and 50th percentiles of all genes were also plotted to set the dynamic range.

In contrast to the case with MMS induction, heat shock-induced genes had comparatively little SWI/SNF and RSC but contained INO80 and ISW1, and their occupancies changed little with heat shock. This comparatively low SWI/SNF enrichment, nevertheless, was similar in magnitude to previous observations, especially at the promoter region, since only the occupancies at the UAS probes were used for the remodelers (38). Thus, classes of genes that respond to distinct environmental stimuli appear to involve the constitutive presence of different but also overlapping sets of chromatin remodeling complexes.

MMS-induced accumulation of Gcn4 at amino acid biosynthetic genes. In addition to DNA, MMS damages proteins (1, 21, 24, 31). Sufficient damage triggers protein turnover and a requirement for additional protein biosynthesis that places demands on the free amino acid pool. MMS treatment is known to induce amino acid biosynthetic genes, which are under the control of Gcn4 (21). We therefore examined whether MMS treatment led to increased occupancy of Gcn4 at the 31 amino acid biosynthetic genes that contain a Gcn4 binding site. We examined Gcn4 occupancy under normal conditions, in the presence of MMS, and also after heat shock (as a control). In

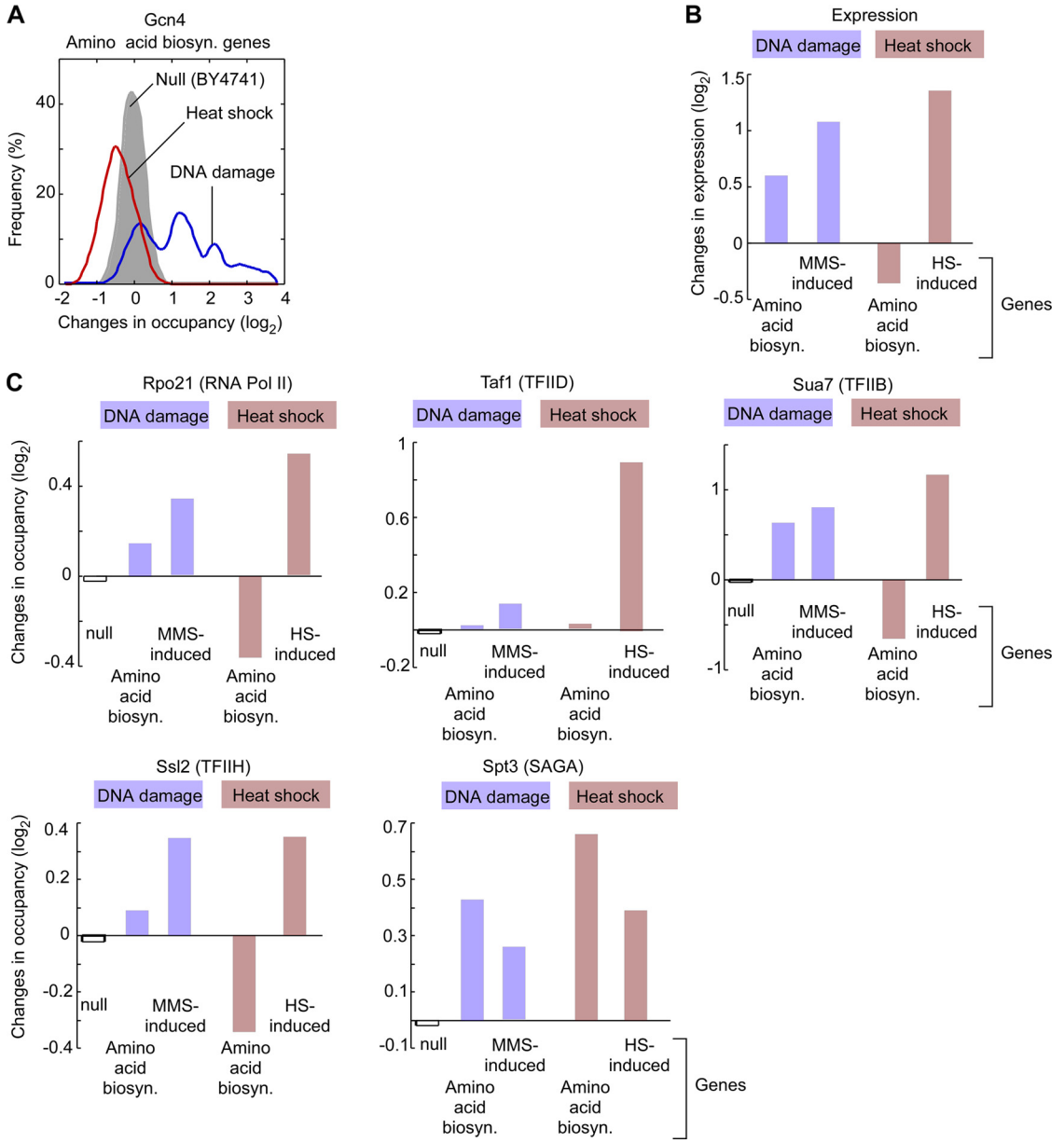

FIG. 7. Increased occupancy of Gcn4 and SAGA at MMS-induced amino acid biosynthetic genes. (A) Frequency distribution plot illustrating changes in occupancy of Gcn4 at the UAS probes in response to heat shock and MMS. (B) Bar graph representing changes in expression of the 31 amino acid biosynthetic genes in response to MMS or heat shock. Changes in expression of MMS- or heat shock-inducible genes (cluster 1 genes from Fig. 1) were used to set the dynamic range. (C) Each panel tracks the indicated GTF and reports the median changes in occupancy in response to MMS or heat shock at the amino acid biosynthetic genes as well as the MMS- or heat shock-inducible (cluster 1) genes.

the presence of MMS, Gcn4 was recruited to most of the 31 genes (Fig. 7A). This level of robust recruitment was not observed during heat shock, demonstrating its specificity toward MMS. As reported previously (21, 31), we also found the expected increase in expression of the amino acid biosynthetic genes in response to MMS treatment but not to heat shock (Fig. 7B). For the 31 genes, we observed preferential recruitment of SAGA (Spt3) and not TFIID (Taf1), consistent with our observations of other MMS-induced genes (Fig. 7C). Thus, Gcn4 is recruited to amino acid biosynthetic genes in response to MMS, likely in response to protein damage, and this leads to assembly of a transcription machinery that likely involves the SAGA complex.

DISCUSSION

Serial versus parallel implementation of the SAGA and TFIID PIC assembly pathways. The goal of this study was to evaluate the similarities and differences in PIC assembly when sets of genes respond to distinct environmental stimuli. The basic question is whether different genes responding to different stimuli set up their PICs in basically the same way. We

found this not to be the case, although commonalities exist. We chose to compare the DNA damage and heat shock responses because prior expression profiling studies suggested that they elicit similar (ESR) as well as distinct stress-specific responses (12, 13). Also, there are differences between the two responses, as one (heat shock response) is transient and the other (DNA damage response) is more prolonged (12).

Previously, we and others reported evidence of two distinct pathways for PIC assembly (19, 22, 25, 29, 39), with one involving the SAGA complex, whose function in TBP delivery tends to predominate at highly regulated stress-induced genes, and the second involving TFIID, whose function in TBP delivery tends to operate at housekeeping genes, which tend to be downregulated in stress. These so called stress-induced and housekeeping genes were originally classified as the inducible and constitutive genes (16, 22, 39). Much work has shown how the inducible genes are more tightly regulated through activators and repressors, whereas the constitutive genes are less dependent on activators. Additionally, studies have shown that for constitutive or housekeeping genes, which are predominantly the TFIID-dominated genes, a mediator is dispensable for TBP recruitment, unlike the case for SAGA-dependent inducible genes (28). Thus, there are variations in PIC assembly at SAGA- versus TFIID-dominated genes, and these may be attributed at least in part to different activators responsible for their activation.

When cells are exposed to an abrupt shift in temperature from 25°C to 37°C, not only do they respond by inducing genes important for stress tolerance, but they also increase their metabolic rates, which necessitates increased expression of metabolic genes (11). Thus, many heat shock-induced genes may be transcriptionally active at 25°C, with higher activity and factor recruitment upon an abrupt shift to 37°C.

Our study does not address interdependencies between SAGA and TFIID. A previous study demonstrated that SAGA is required for TFIID recruitment (42) to the hexose transporter genes *HXT2* and *HXT4*, which is consistent with the temporal profile shown here. Another study demonstrated that *RNR3* induction by MMS is dependent upon both SAGA and TFIID (51). On a genomic scale, genes depend on both TFIID and SAGA, to various extents (19, 25). Taken together, the evidence supports the notion that SAGA is present early in an activation response, where it appears to be involved in histone acetylation and TBP recruitment.

SAGA may promote rapid PIC assembly in response to stress, whereas the timing of the response through TFIID may be more stimulus specific, with heat stress creating a rapid response and DNA damage creating a slower but more sustained response. Heat shock genes tend to be more functionally dependent on SAGA than on TFIID, perhaps because the response is so transient that the contribution from TFIID is not fully realized. MMS-induced genes tend to be more TFIID dominated, despite the presence of SAGA, perhaps because the SAGA contribution to PIC assembly is rather short and the TFIID contribution is rather prolonged during sustained activation of these genes. Once the TFIID pathway takes charge, the presence of SAGA may not be required (at least for PIC assembly).

Conceivably, genes that are regulated to have their assembly pathways in constant flux, from highly repressed to highly activated, may be more SAGA dominated due to the rapidity with which SAGA can promote transient PIC assembly compared to the slower TFIID recruitment, and possibly slower TFIID-directed PIC assembly. However, slower TFIID recruitment may be gene specific or specific for types of environmental responses rather than an inherent limitation of TFIID, in that recruitment is rapid at heat shock-induced genes. Thus, a loss of TFIID would have less of an impact than a loss of SAGA for high-flux genes. Genes that are regulated by a more sustained recruitment of the PIC may nevertheless recruit both SAGA and TFIID, but a long-lived presence of TFIID might be manifested by a greater dependence on it.

Both heat shock and DNA damage induce a common set of about 25 genes, based upon the stringent filtering criteria used in our study. In regard to the timing of SAGA/TFIID recruitment, they followed the MMS-induced serial recruitment pattern when responding to MMS but followed the heat shock-induced parallel pattern when responding to heat shock (data not shown). Thus, the type of environmental stress and, by implication, the respective stress-specific signal transduction cascade may dictate the predominant PIC assembly pathway (and timing) for a given gene.

Thus far, studies have shown how cells exposed simultaneously to two different stress conditions, such as hypo-osmotic shock along with mild heat shock, show a combined genomic response, which is usually a sum of both responses (14). This shows how efficiently cells can respond independently to two different conditions simultaneously and is another example of how multiple diverse regulatory pathways orchestrate a response to a distinct environmental condition. It would therefore be interesting to study PIC assembly under varied stress conditions, independently as well as in combination, to dissect all of the complex mechanisms employed by cells to ensure survival.

Apart from *RNR* genes, Crt1 does not play a widespread role at DNA damage-inducible genes. Our finding that Crt1 is not present at MMS-inducible genes, except for *RNR* genes, was surprising because the notion that Crt1 negatively regulates the *RNR* genes has been a model for DNA damage-inducible gene regulation. One question that remains to be addressed is what other factors (if any) play a role in repression of those genes under normal growth conditions. Additionally, if Crt1 does not bind to DNA damage-inducible genes, then what common thread links it to the genes to which it does bind?

Constitutive presence of chromatin remodeling complexes. We found that both heat shock- and DNA damage-inducible genes involve multiple chromatin remodeling complexes that appear to be constitutively present before and after induction. The two classes of genes utilize the same and different chromatin remodeling complexes. While the basis for this distinction is unclear, differential use of chromatin remodelers might be related to lower levels of uninduced expression in one class versus the other, or it may be related to transient versus sustained induction, perhaps in some way linked to serial versus parallel use of the SAGA and TFIID PIC assembly pathways.

ACKNOWLEDGMENTS

We thank J. Reese for many helpful suggestions. We thank I. Albert, C. Jiang, and G. S. Chang for bioinformatic support, including map-

ping of sequencing tags. The SOLiD sequencing described here was performed at the Penn State Nucleic Acid Facility.

This work was supported by NIH grant ES013768. This project was funded in part under a grant from the Pennsylvania Department of Health, using tobacco settlement funds.

The Pennsylvania Department of Health specifically disclaims responsibility for any analyses, interpretations, or conclusions presented here.

REFERENCES

1. **Boffa, L. C., and C. Bolognesi.** 1985. Nuclear proteins damage by alkylating agents with different degrees of carcinogenicity. Chem. Biol. Interact. **55:** 235–245.
2. **Brown, C. E., L. Howe, K. Sousa, S. C. Alley, M. J. Carrozza, S. Tan, and J. L. Workman.** 2001. Recruitment of HAT complexes by direct activator interactions with the ATM-related Tra1 subunit. Science **292:**2333–2337.
3. **Cairns, B. R.** 2004. Around the world of DNA damage INO80 days. Cell **119:**733–735.
4. **Causton, H. C., B. Ren, S. S. Koh, C. T. Harbison, E. Kanin, E. G. Jennings, T. I. Lee, H. L. True, E. S. Lander, and R. A. Young.** 2001. Remodeling of yeast genome expression in response to environmental changes. Mol. Biol. Cell **12:**323–337.
5. **Chitikila, C., K. L. Huisinga, J. D. Irvin, A. D. Basehoar, and B. F. Pugh.** 2002. Interplay of TBP inhibitors in global transcriptional control. Mol. Cell **10:**871–882.
6. **D'Alessio, J. A., K. J. Wright, and R. Tjian.** 2009. Shifting players and paradigms in cell-specific transcription. Mol. Cell **36:**924–931.
7. **Drysdale, C. M., B. M. Jackson, R. McVeigh, E. R. Klebanow, Y. Bai, T. Kokubo, M. Swanson, Y. Nakatani, P. A. Weil, and A. G. Hinnebusch.** 1998. The Gcn4p activation domain interacts specifically in vitro with RNA polymerase II holoenzyme, TFIID, and the Adap-Gcn5p coactivator complex. Mol. Cell. Biol. **18:**1711–1724.
8. **Eisen, M. B., P. T. Spellman, P. O. Brown, and D. Botstein.** 1998. Cluster analysis and display of genome-wide expression patterns. Proc. Natl. Acad. Sci. U. S. A. **95:**14863–14868.
9. **Elledge, S. J., Z. Zhou, J. B. Allen, and T. A. Navas.** 1993. DNA damage and cell cycle regulation of ribonucleotide reductase. Bioessays **15:**333–339.
10. **Fishburn, J., N. Mohibullah, and S. Hahn.** 2005. Function of a eukaryotic transcription activator during the transcription cycle. Mol. Cell **18:**369–378.
11. **Gasch, A. P.** 2007. Comparative genomics of the environmental stress response in ascomycete fungi. Yeast **24:**961–976.
12. **Gasch, A. P., M. Huang, S. Metzner, D. Botstein, S. J. Elledge, and P. O. Brown.** 2001. Genomic expression responses to DNA-damaging agents and the regulatory role of the yeast ATR homolog Mec1p. Mol. Biol. Cell **12:**2987–3003.
13. **Gasch, A. P., P. T. Spellman, C. M. Kao, O. Carmel-Harel, M. B. Eisen, G. Storz, D. Botstein, and P. O. Brown.** 2000. Genomic expression programs in the response of yeast cells to environmental changes. Mol. Biol. Cell **11:** 4241–4257.
14. **Gasch, A. P., and M. Werner-Washburne.** 2002. The genomics of yeast responses to environmental stress and starvation. Funct. Integr. Genomics **2:**181–192.
15. **Harbison, C. T., D. B. Gordon, T. I. Lee, N. J. Rinaldi, K. D. Macisaac, T. W. Danford, N. M. Hannett, J. B. Tagne, D. B. Reynolds, J. Yoo, E. G. Jennings, J. Zeitlinger, D. K. Pokholok, M. Kellis, P. A. Rolfe, K. T. Takusagawa, E. S. Lander, D. K. Gifford, E. Fraenkel, and R. A. Young.** 2004. Transcriptional regulatory code of a eukaryotic genome. Nature **431:**99–104.
16. **Harbury, P. A., and K. Struhl.** 1989. Functional distinctions between yeast TATA elements. Mol. Cell. Biol. **9:**5298–5304.
17. **Holstege, F. C., E. G. Jennings, J. J. Wyrick, T. I. Lee, C. J. Hengartner, M. R. Green, T. R. Golub, E. S. Lander, and R. A. Young.** 1998. Dissecting the regulatory circuitry of a eukaryotic genome. Cell **95:**717–728.
18. **Huang, M., Z. Zhou, and S. J. Elledge.** 1998. The DNA replication and damage checkpoint pathways induce transcription by inhibition of the Crt1 repressor. Cell **94:**595–605.
19. **Huisinga, K. L., and B. F. Pugh.** 2004. A genome-wide housekeeping role for TFIID and a highly regulated stress-related role for SAGA in Saccharomyces cerevisiae. Mol. Cell **13:**573–585.
20. **Jelinsky, S. A., P. Estep, G. M. Church, and L. D. Samson.** 2000. Regulatory networks revealed by transcriptional profiling of damaged Saccharomyces cerevisiae cells: Rpn4 links base excision repair with proteasomes. Mol. Cell. Biol. **20:**8157–8167.
21. **Jelinsky, S. A., and L. D. Samson.** 1999. Global response of Saccharomyces cerevisiae to an alkylating agent. Proc. Natl. Acad. Sci. U. S. A. **96:**1486–1491.
22. **Kuras, L., P. Kosa, M. Mencia, and K. Struhl.** 2000. TAF-containing and TAF-independent forms of transcriptionally active TBP in vivo. Science **288:**1244–1248.
23. **Larschan, E., and F. Winston.** 2001. The S. cerevisiae SAGA complex functions in vivo as a coactivator for transcriptional activation by Gal4. Genes Dev. **15:**1946–1956.
24. **Lee, M. Y., M. A. Kim, H. J. Kim, Y. S. Bae, J. I. Park, J. Y. Kwak, J. H. Chung, and J. Yun.** 2007. Alkylating agent methyl methanesulfonate (MMS) induces a wave of global protein hyperacetylation: implications in cancer cell death. Biochem. Biophys. Res. Commun. **360:**483–489.
25. **Lee, T. I., H. C. Causton, F. C. Holstege, W. C. Shen, N. Hannett, E. G. Jennings, F. Winston, M. R. Green, and R. A. Young.** 2000. Redundant roles for the TFIID and SAGA complexes in global transcription. Nature **405:** 701–704.
26. **Lee, T. I., N. J. Rinaldi, F. Robert, D. T. Odom, Z. Bar-Joseph, G. K. Gerber, N. M. Hannett, C. T. Harbison, C. M. Thompson, I. Simon, J. Zeitlinger, E. G. Jennings, H. L. Murray, D. B. Gordon, B. Ren, J. J. Wyrick, J. B. Tagne, T. L. Volkert, E. Fraenkel, D. K. Gifford, and R. A. Young.** 2002. Transcriptional regulatory networks in Saccharomyces cerevisiae. Science **298:**799–804.
27. **Li, B., and J. C. Reese.** 2001. Ssn6-Tup1 regulates RNR3 by positioning nucleosomes and affecting the chromatin structure at the upstream repression sequence. J. Biol. Chem. **276:**33788–33797.
28. **Li, X. Y., S. R. Bhaumik, and M. R. Green.** 2000. Distinct classes of yeast promoters revealed by differential TAF recruitment. Science **288:**1242–1244.
29. **Mencia, M., Z. Moqtaderi, J. V. Geisberg, L. Kuras, and K. Struhl.** 2002. Activator-specific recruitment of TFIID and regulation of ribosomal protein genes in yeast. Mol. Cell **9:**823–833.
30. **Morrison, A. J., J. A. Kim, M. D. Person, J. Highland, J. Xiao, T. S. Wehr, S. Hensley, Y. Bao, J. Shen, S. R. Collins, J. S. Weissman, J. Delrow, N. J. Krogan, J. E. Haber, and X. Shen.** 2007. Mec1/Tel1 phosphorylation of the INO80 chromatin remodeling complex influences DNA damage checkpoint responses. Cell **130:**499–511.
31. **Natarajan, K., M. R. Meyer, B. M. Jackson, D. Slade, C. Roberts, A. G. Hinnebusch, and M. J. Marton.** 2001. Transcriptional profiling shows that Gcn4p is a master regulator of gene expression during amino acid starvation in yeast. Mol. Cell. Biol. **21:**4347–4368.
32. **Ohtsuki, K., K. Kasahara, K. Shirahige, and T. Kokubo.** 2010. Genome-wide localization analysis of a complete set of Tafs reveals a specific effect of the Taf1 mutation on Taf2 occupancy and provides indirect evidence for different TFIID conformations at different promoters. Nucleic Acids Res. **38:**1805–1820.
33. **Orphanides, G., and D. Reinberg.** 2002. A unified theory of gene expression. Cell **108:**439–451.
34. **Ren, B., F. Robert, J. J. Wyrick, O. Aparicio, E. G. Jennings, I. Simon, J. Zeitlinger, J. Schreiber, N. Hannett, E. Kanin, T. L. Volkert, C. J. Wilson, S. P. Bell, and R. A. Young.** 2000. Genome-wide location and function of DNA binding proteins. Science **290:**2306–2309.
35. **Rumble, S. M., P. Lacroute, A. V. Dalca, M. Fiume, A. Sidow, and M. Brudno.** 2009. SHRiMP: accurate mapping of short color-space reads. PLoS Comput. Biol. **5:**e1000386.
36. **Sharma, V. M., B. Li, and J. C. Reese.** 2003. SWI/SNF-dependent chromatin remodeling of RNR3 requires TAF(II)s and the general transcription machinery. Genes Dev. **17:**502–515.
37. **Sharma, V. M., R. S. Tomar, A. E. Dempsey, and J. C. Reese.** 2007. Histone deacetylases RPD3 and HOS2 regulate the transcriptional activation of DNA damage-inducible genes. Mol. Cell. Biol. **27:**3199–3210.
38. **Shivaswamy, S., and V. R. Iyer.** 2008. Stress-dependent dynamics of global chromatin remodeling in yeast: dual role for SWI/SNF in the heat shock stress response. Mol. Cell. Biol. **28:**2221–2234.
39. **Struhl, K.** 1986. Constitutive and inducible Saccharomyces cerevisiae promoters: evidence for two distinct molecular mechanisms. Mol. Cell. Biol. **6:**3847–3853.
40. **Struhl, K., D. Kadosh, M. Keaveney, L. Kuras, and Z. Moqtaderi.** 1998. Activation and repression mechanisms in yeast. Cold Spring Harb. Symp. Quant Biol. **63:**413–421.
41. **Swanson, M. J., H. Qiu, L. Sumibcay, A. Krueger, S. J. Kim, K. Natarajan, S. Yoon, and A. G. Hinnebusch.** 2003. A multiplicity of coactivators is required by Gcn4p at individual promoters in vivo. Mol. Cell. Biol. **23:**2800–2820.
42. **van Oevelen, C. J., H. A. van Teeffelen, and H. T. Timmers.** 2005. Differential requirement of SAGA subunits for Mot1p and Taf1p recruitment in gene activation. Mol. Cell. Biol. **25:**4863–4872.
43. **Venters, B. J., and B. F. Pugh.** 2009. A canonical promoter organization of the transcription machinery and its regulators in the Saccharomyces genome. Genome Res. **19:**360–371.
44. **Venters, B. J., and B. F. Pugh.** 2009. How eukaryotic genes are transcribed. Crit. Rev. Biochem. Mol. Biol. **44:**117–141.
45. **Wahl, G. M., and A. M. Carr.** 2001. The evolution of diverse biological responses to DNA damage: insights from yeast and p53. Nat. Cell Biol. **3:**E277–E286.
46. **Weinert, T.** 1998. DNA damage and checkpoint pathways: molecular anatomy and interactions with repair. Cell **94:**555–558.
47. **Workman, C. T., H. C. Mak, S. McCuine, J. B. Tagne, M. Agarwal, O. Ozier, T. J. Begley, L. D. Samson, and T. Ideker.** 2006. A systems approach to mapping DNA damage response pathways. Science **312:**1054–1059.
48. **Zaim, J., E. Speina, and A. M. Kierzek.** 2005. Identification of new genes

regulated by the Crt1 transcription factor, an effector of the DNA damage checkpoint pathway in Saccharomyces cerevisiae. J. Biol. Chem. **280:**28–37.
49. **Zanton, S. J., and B. F. Pugh.** 2004. Changes in genomewide occupancy of core transcriptional regulators during heat stress. Proc. Natl. Acad. Sci. U. S. A. **101:**16843–16848.
50. **Zanton, S. J., and B. F. Pugh.** 2006. Full and partial genome-wide assembly and disassembly of the yeast transcription machinery in response to heat shock. Genes Dev. **20:**2250–2265.
51. **Zhang, H., J. A. Kruk, and J. C. Reese.** 2008. Dissection of coactivator requirement at RNR3 reveals unexpected contributions from TFIID and SAGA. J. Biol. Chem. **283:**27360–27368.
52. **Zhang, H., and J. C. Reese.** 2007. Exposing the core promoter is sufficient to activate transcription and alter coactivator requirement at RNR3. Proc. Natl. Acad. Sci. U. S. A. **104:**8833–8838.
53. **Zhang, Z., and J. C. Reese.** 2005. Molecular genetic analysis of the yeast repressor Rfx1/Crt1 reveals a novel two-step regulatory mechanism. Mol. Cell. Biol. **25:**7399–7411.
54. **Zhou, B. B., and S. J. Elledge.** 2000. The DNA damage response: putting checkpoints in perspective. Nature **408:**433–439.
55. **Zhou, Z., and S. J. Elledge.** 1992. Isolation of crt mutants constitutive for transcription of the DNA damage inducible gene RNR3 in Saccharomyces cerevisiae. Genetics **131:**851–866.